



## Original article

## Study on volume reduction of radioactive perlite thermal insulation waste by heat treatment with potassium carbonate

Yi-Sin Chou <sup>a</sup>, Bhupendra Singh <sup>b</sup>, Yong-Song Chen <sup>b,\*</sup>, Shi-Chern Yen <sup>c</sup><sup>a</sup> Chemical Engineering Division, Institute of Nuclear Energy Research, Longtan, Taoyuan 32546, Taiwan<sup>b</sup> Department of Mechanical Engineering and Advanced Institute of Manufacturing with High-tech Innovations, National Chung Cheng University, Minhsiung Township, Chiayi County 62102, Taiwan<sup>c</sup> Department of Chemical Engineering, National Taiwan University, Taipei 10617, Taiwan

## ARTICLE INFO

## Article history:

Received 2 March 2021

Received in revised form

7 July 2021

Accepted 16 July 2021

Available online 16 July 2021

## Keywords:

Perlite

Radioactive thermal insulation waste

Volume reduction ratio

High-temperature sintering

Potassium carbonate flux

## ABSTRACT

Perlite is one of the major constituents of the radioactive thermal insulation waste (RTIW) originating from nuclear power plants and, for proper waste management, a significant reduction in its volume is required prior to disposal. In this work, the volume reduction of perlite is studied by high-temperature treatment method with using  $K_2CO_3$  as a flux. The perlite is ground with 0–30 wt%  $K_2CO_3$ , and differential thermal analysis/thermogravimetric analysis is used to monitor the glass transition temperature ( $T_g$ ) and weight loss. The  $T_g$  varied between  $\sim 772.2$  and  $837.1$  °C with the minima at  $\sim 643.5$  °C with the addition of  $\sim 10$  wt%  $K_2CO_3$ . It is observed that compared to the pure perlite the volume reduction ratio (VRR) increases with the addition of  $K_2CO_3$ . The VRR of 11.20 is observed with 5 wt%  $K_2CO_3$  at 700 °C, as compared to VRR of 5.56 without  $K_2CO_3$  at 700 °C. The X-ray photoelectron spectroscopy and scanning electron microscopy are used to characterize perlite samples heat-treated without/with 5 wt%  $K_2CO_3$  at 700 °C. Moreover, the atomic absorption spectroscopy indicates that the proposed heat-treatment procedure is able to completely retain the radionuclides present in the perlite RTIW.

© 2021 Korean Nuclear Society, Published by Elsevier Korea LLC. This is an open access article under the CC BY-NC-ND license (<http://creativecommons.org/licenses/by-nc-nd/4.0/>).

## 1. Introduction

Given the human safety and environmental impact are the most important concern in the treatment of nuclear waste, the operations for the management of the primary radioactive waste (RW) are intended to address these concerns while keeping the economics in mind. The RW include materials that are either intrinsically radioactive or have been contaminated by radioactivity. Based on their level of radioactivity, the waste is classified as low-level waste, intermediate-level waste, and high-level waste. The low-level waste has a radioactive content  $<4$  Bq/g of alpha activity or 12 Bq/g beta-gamma activity, they do not require shielding during handling and transport, and are suitable for disposal in near-surface facilities [1]. Therefore, for low-level solid nuclear waste, which mainly consists of waste paper, cloths, tools, thermal insulations, etc., the main purpose of the waste-treatment is volume reduction and the options for this are compression, incineration and pyrolysis, melting, and

decomposition (chemical/thermal/biochemical) [2]. Accordingly, volume reduction, removal of radionuclides, and change of physical state and chemical composition have been the main objectives of nuclear waste treatment and conditioning [2]. The nuclear power plants use a large amount of thermal insulation materials such as mineral wool, expanded perlite, calcium silicates, fiberglass, and urethane and polyurethane foam, and aluminosilicate-based construction materials such as concrete, plasters, and bricks [3,4]. Thus, planned measures for decommissioning of nuclear power plants are bound to create a large amount of RW to be disposed of. In the future, volume reduction methods should be developed to increase the storage capacity, while avoiding the need for continuous treatment after nuclear power plants are decommissioned. The most common method for volume reduction of low-level radioactive thermal insulation waste (RTIW) from nuclear power plants is compaction which involves using sacrificial barrels to contain waste materials and compressing with  $\sim 10$ – $50$  ton force for compaction or with  $\sim 1000$ – $2000$  ton force for super-compaction [5]. Before and after super-compressing insulation material, it uses the filling in the same disposal barrel to determine the volume reduction ratio of the insulation materials [6]. Depending upon the characteristics of

\* Corresponding author.

E-mail address: [imeysc@ccu.edu.tw](mailto:imeysc@ccu.edu.tw) (Y.-S. Chen).

the waste material, the volume reduction ratio (VRR) of ~2–5 during compaction and ~100 during super-compaction is achieved [2]. However, after long-term storage, the sacrificial barrel will have the risk of expansion and corrosion, which will damage the sacrificial barrel and cause the release of waste insulation materials.

The application of thermal technologies for the treatment and conditioning of the low-level radioactive thermal insulation waste (LLRTIW) is another way leading to the volume reduction and involves high-temperature incineration (HTI), thermochemical treatment, melting, and plasma treatment [7]. The HTI is used when organic materials are present in RTIW and a VRR of ~3–5 can be achieved with HTI, however, this method is very sensitive to waste composition, and sometimes presorting of the waste is required. The thermochemical treatment uses powdered metal fuels that are specifically formulated for the waste composition and react exothermically with the waste components. The radionuclides are mostly volatilized and subsequently trapped in the produced metal slag. Although this method eliminates many of the challenges associated with most other thermal technologies, this requires special care to manage the hydrogen produced during the exothermic reaction. On the other hand, melting involves applying enough heat to melt the waste components into liquid material which is poured into molds and allowed to cool. The elimination of void spaces and the resultant increase in density leads to volume reduction with a VRR of ~5–20, however, it is limited mainly to metallic waste and requires temperatures >1300 °C and extensive presorting as the melting of mixed metal components is normally not economical for the low-level RTIW [7]. Molten salt oxidation (MSO), a flameless thermal desorption process where the RW is introduced into a bath of molten salts at temperatures ~500–950 °C, is used for the treatment of the RW containing organic material and efficiently captures ash and radioactive particles within the salt bath. The lower operating temperature compared to other thermal technologies has generated significant interest [8,9] and recently an advancement to MSO, catalyst enhanced MSO [10,11] have been proposed. Moreover, another method involving high-temperature vitrification has been also employed to solidify RW with glass. The solidified material has good physical and chemical durability for long-term storage, transportation and subsequent disposal operations. However, due to the high cost of high-temperature operation, at present this is mostly used for the high-level RW [7]. For the heating methods to effectively process the LLRTIW, a high level of combustibles components is desirable, but the major components of the LLRTIW are non-combustible substances. Plasma heating using plasma torches, which provides a high degree of concentration of the thermal energy in the plasma jet and can achieve temperatures of several thousand °C, can treat any type of inorganic/mixed LLRTIW, requires high electrical power to generate plasma arc. The torch is easy to be destroyed and currently the method is tested only in limited facilities.

An important motivation for this study is the Taiwan government's aim to phase out all nuclear power plants by year 2025 [12], which will result in a huge quantity and volume of waste radioactive insulation materials. The main sources of the low-level radioactive insulation material waste generated during the decommissioning of the first nuclear power plant in Taiwan are the insulation materials covering the periphery of the pressure tank of the nuclear reactor and the surface of the pipeline, such as perlite, rock wool, glass fiber, etcetera [13,14]. In Taiwan, perlite accounts for nearly 50% of the low-level RTIW and a total of 7000 55-gallon (208 L) drums are stored after the decommissioning of the nuclear power plant [13]. Since the composition of different insulation materials is very different, it is planned to classify and

then reduce the volume. Raw perlite is a siliceous rock originating from pumice, a glassy form of rhyolitic or dacitic magma, and contains a small amount (2–6%) of bound water. Upon rapid heating at high temperatures, the bound water boils. The resultant steam forms bubbles, in the form of sealed glassy cells resembling popcorns, within the softened rock cause the perlite to expand 4–20 times of its initial volume [15,16]. A great degree of variation about the temperature affecting the abovementioned transformation is reported in literature [15–20], with as low as 760–900 °C [17] to as high as 850–1150 °C [18]. Nevertheless, this makes the perlite highly porous and lightweight material with excellent thermal insulating and construction material properties. The binary/ternary mixtures of alkali metal carbonates have been extensively used as a molten salt bath in MSO process [7,8] and there are a few old reports of using these as a constituent in the binary fusion flux mixture with boric acid, alkali metal tetraborates/metaborates for the fusion of silicates at >1000 °C [21–23]. The phase diagram of potassium oxide and silicon dioxide has an eutectic point at 772 °C, turning it into a liquid if at the corresponding concentrations and heated to that temperature [24]. In this way, heat-insulating materials containing a high proportion of silicon dioxide have a chance to achieve high-temperature sintering. The <sup>60</sup>Co is one of the important radionuclides produced by neutron activation reactions and present as a contaminant in the thermal and electrical insulations during the decommissioning of the nuclear power plants [25,26], as the mechanical components of nuclear power plants use cobalt-containing materials to enhance the mechanical strength. When the module with the cobalt content is exposed to high-radiation environments for a long time, it would be aged and corroded, while the component breaks down and splits into pollutants and Co would transform into the isomer, <sup>60m</sup>Co [27]. The heat-insulating material wrapped on the outside will be contaminated by falling off pollutants. The metal substance contained in perlite comes from its own mineral composition and foaming agent. In the central reaction position of the nuclear reactor, neutron impact causes a chain reaction to release heat [28]. The location of the insulation material has a low chance of contacting neutrons, and the material itself cannot produce the pollution of the fission products.

Therefore, based on the aforesaid observations, in this work the volume reduction of perlite, which is a major constituent of many LLRTIW, is studied by high-temperature melting method while using potassium carbonate (K<sub>2</sub>CO<sub>3</sub>) as a flux. For this purpose, the thermal analysis is used to monitor the glass transition temperature and weight loss, and X-ray Photoelectron Spectroscopy (XPS), Scanning Electron Microscopy (SEM) and Energy Dispersive X-ray Spectroscopy (EDS) are used to analyze the chemical and microstructural changes taking place due to the heat-treatment. Moreover, Atomic absorption spectroscopy (AAS) is used to analyze the <sup>60</sup>Co-retention ability of the heated perlite.

## 2. Experimental

All chemicals including perlite, K<sub>2</sub>CO<sub>3</sub> (Alfa Aesar, 99.0%), and Co(NO<sub>3</sub>)<sub>2</sub>·6H<sub>2</sub>O (Sigma Aldrich, ≥98.0%) were of analytical grade and were used without purification. Uniform mixtures of perlite and K<sub>2</sub>CO<sub>3</sub>, in different weight ratios, were prepared by grinding using mortar and pestle. The effect of heat-treatment on thermogravimetry of various samples was studied using thermogravimetric analyzer (DTA/TGA; NETZSCH, STA449 F3) by heating in an alumina crucible from room temperature to 1050 °C range in N<sub>2</sub> atmosphere with heating rate of 20 K/min.

The waste VRR, defined as the ratio of the initial volume of the treated waste ( $V_i$ ) to the final volume after the treatment ( $V_f$ ), was

calculated using Eq. (1) [2].

$$VRR = \frac{V_f}{V_i} \quad (1)$$

The  $V_i$  or  $V_f$  were calculated as follows: First the weight of perlite was soaked in water, then placed in a 20 ml measuring bottle (weight of empty bottle,  $W_b$ ) and weight ( $W_1$ ) was measured. The bottle was filled with water and overall weight ( $W_2$ ) was measured. The weight difference ( $W_2 - W_1$ ) was the volume ( $V_{wp}$ ) of water filled in the bottle in the presence of perlite. The perlite was removed and the bottle was filled again by adding additional water. The weight ( $W_{b+w}$ ) of the water filled bottle was measured. The difference ( $W_{b+w} - W_b$ ) was the volume of water ( $V_w$ ) that can be filled in the bottle in the absence of perlite. Finally, the difference ( $V_w - V_{wp}$ ) was the volume of the perlite.

The surface morphology of the perlite before and after the heat-treatment with/without  $K_2CO_3$  was analyzed by Scanning Electron Microscopy (SEM) using a field emission scanning electron microscope (FESEM; Hitachi, S4800). In addition, this machine was also equipped with Energy Dispersive X-ray Spectroscopy (EDS) for semi-quantitative analysis of elements.

X-ray photoelectron spectroscopy (XPS) was performed using X-ray photoelectron spectrometer (XPS/PHI, Quantera SXM). The binding energies of C 1s, O 1s, Si 2p, Na 1s, Al 2p, and K 2p photoelectron peaks were determined and the chemical composition was investigated on the basis of peak areas.

Atomic absorption spectroscopy was performed to analyze the retention of cobalt in the heated perlite. Before AAS experiments, the perlite and  $K_2CO_3$  flux were ground using agate mortar and pestle into powder, then added 37.6 ppm equivalent of Co, used as the simulated radionuclide, in the form of  $Co(NO_3)_2 \cdot 6H_2O$  in 100 ml deionized water. Microwave heating treatment was performed for 1 h, after the solution was cooled, the separated precipitate was washed several times with deionized water, and dried in an oven. The insulation materials were heat-treated at 95 °C in 50 ml of 6 N nitric acid. By nitrification, the insulation material with cobalt ion content would dissolve and form  $Co(NO_3)_2 \cdot 6H_2O$ . The nitrified insulation material was filtered to remove the filtrate. After many nitrifying operations, it was ensured that the precipitate did not contain cobalt ions, and the cobalt content of the insulation material was completely extracted. The extraction liquid obtained from the digestion of the insulation material and the gasified extract was used to measure the absorption spectrum of cobalt to determine the cobalt concentration. The absorption spectroscopy analysis was performed to remove background interference at 1200 °C [29]. A flame Atomic Absorption Spectrometer (AAS; PerkinElmer, PinAAcle 900F) equipped with a graphite furnace with acetylene burner and having a hollow cathode tube to contain the metal element to be measured, was used for the AAS analysis. The measurement wavelength range (190–800 nm) was selected, based on the absorbance wavelength of the atom under study, by a single optical device and the experiment time was about 3–10 s. The absorbance data was then converted to calculate the concentration of the metal element to be measured in the sample, with the accuracy of 0.01 ppm.

### 3. Results and discussion

In the present work, we study the effect of heat-treatment on the volume reduction of perlite, supposed to be originating as an insulation and construction waste from the nuclear power plants, while using  $K_2CO_3$  as a flux. The perlite is grinded with 0–30 wt%  $K_2CO_3$ , and the thermogravimetric analysis is used to monitor the glass transition temperature. Firstly, the effect of the addition of

$K_2CO_3$  flux on the glass transition temperature was studied by adding 0–30 wt%  $K_2CO_3$  in 30 ml of perlite powder. The addition of  $K_2CO_3$  increases the entropy of the mixture and the resulting enthalpy change observed during DTA is also positive. Accordingly, the  $T_g$  calculated from the DTA is plotted in Fig. 1(a). As can be seen, the  $T_g$  varies between ~772.2 and 837.1 °C with the addition of 0–30 wt% of  $K_2CO_3$ . Firstly,  $T_g$  decreases to ~643.5 °C with the addition of 0–10 wt% but then increases with further addition of 10–30 wt%  $K_2CO_3$ . The weight retention rate in TGA with the addition of 0–10 wt%  $K_2CO_3$  is shown in Fig. 1(b). As can be seen, the heat-treatment reduces the overall weight by 7–20%, depending upon the amount of  $K_2CO_3$  added. The release of hydroxyl groups [17] and carbonization reaction occurs in 350–550 °C range and there is very little weight loss in the glass transition range, except for the sample containing 10 wt%  $K_2CO_3$ . In the carbonization range (350–550 °C), the organic compounds contained in perlite decomposes to form carbon dioxide [7]. Moreover, the water present in perlite is gradually driven out upon heating over a wide range of temperatures from 140 to 700 °C up to the glass transition temperature, which could be the cause of the additional weight loss in 550–675 °C range [30,31]. Although the minimum value of  $T_g$  was observed ~8 wt%  $K_2CO_3$ , in Fig. 1(a), the amount of  $K_2CO_3$  was taken at 10 wt%, as it was expected that with 10 wt%  $K_2CO_3$  the theoretical ratio of K/Si will be close to that in  $K_2O-SiO_2$  eutectic mixture derived from  $K_2CO_3+SiO_2$  mixture [24]. It was observed that compared to the perlite the mixture shows a negative deviation in the glass transition temperature and causes higher reduction in the waste volume.

To monitor the volume reduction, different amounts of  $K_2CO_3$  were separately mixed with 30 ml perlite. The parts of the mixture

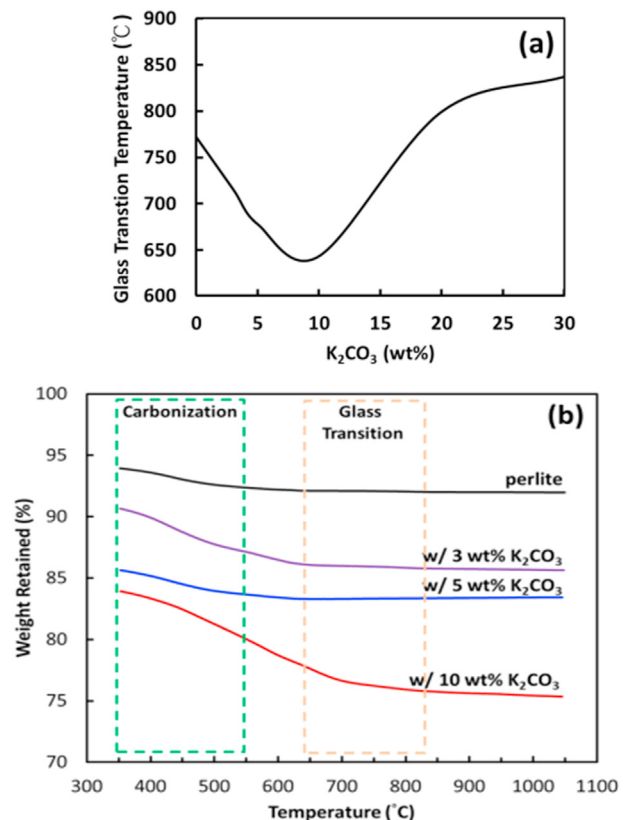


Fig. 1. (a) Glass transition temperature and (b) weight retention of perlite with  $K_2CO_3$  recorded by TGA.

**Table 1**  
VRR of perlite heat-treated at different temperatures with the addition of different wt.% of  $K_2CO_3$ .

Temperature (°C)	VRR with different wt.% of $K_2CO_3$ addition			
	0 wt%	3 wt%	5 wt%	10 wt%
650	4.12	–	–	6.54
675	–	–	7.63	6.99
700	5.56	8.00	11.20	10.00
800	7.14	–	–	10.04
900	8.33	–	–	10.10

were separately kept at different temperatures in a tubular furnace in  $N_2$  atmosphere for 2 h. The waste VRR calculated using Eq. (1) is given in Table 1. As can be seen, compared to the pure perlite the VRR increases with the addition of  $K_2CO_3$ . Moreover, the VRR with 5 wt% were 7.63 and 11.20 at 675 °C and 700 °C whereas the corresponding values with 10 wt% were 6.99 and 10.00, indicating that although the addition of 10 wt%  $K_2CO_3$  leads to a greater drop in  $T_g$  and greater weight loss compared to the addition of 5 wt%  $K_2CO_3$ , the maximum VRR in 650–700 °C range is observed with the addition of 5 wt%  $K_2CO_3$ . Additionally, the VRR for perlite sample without flux increases significantly along with the increasing temperature beyond 700 °C, no significant increase in VRR is observed for the perlite with 10 wt%  $K_2CO_3$ . At the present, it is difficult to exactly predict the mechanism of action of  $K_2CO_3$  flux in volume reduction, very little change in VRR beyond 700 °C, a temperature above the  $T_g$ , may indicate that the volume reduction effect of  $K_2CO_3$  flux is closely related with the glass transition.

The chemical composition of perlite is reported earlier in literature and the main constituents are  $SiO_2$ ,  $Al_2O_3$ ,  $Na_2O$ ,  $K_2O$ ,  $CaO$ ,  $Fe_2O_3$ , and water [23,26,32,33]. XPS and EDS were performed to analyze the elemental composition of the perlite samples heat-treated at 700 °C without/with  $K_2CO_3$  flux. The XPS data for the perlite samples heat-treated without and with 5 wt%  $K_2CO_3$  flux is shown in Fig. 2(a) and (c) respectively whereas the EDS data for the perlite samples heat-treated without and with 5 wt%  $K_2CO_3$  flux is shown in Fig. 2(b) and (d), respectively. The surface elemental composition was calculated on the basis of XPS peak areas and is summarized in Table 2. The occurrence of the C 1s and N 1s peaks are due to the contamination, the presence of a high proportion of C 1s peaks can be attributed to a higher organic component in the perlite sample, as was also visible from the carbonation reaction in TGA data in Fig. 1(b), although a high proportion of C 1s peaks in the XPS data of perlite is not unusual [33]. In the sample with 5 wt%  $K_2CO_3$ , the increase in the atomic percentage of K was expected, however the higher percentage of O but a lower percentage of C is interesting, presuming that the contribution of C from the instrument will be the same for both samples (with/without  $K_2CO_3$ ). This can be explained on the basis of the very nature of  $K_2CO_3$  as a flux that causes greater oxidation of carbonaceous materials thus lowering the C content. Moreover, because the XPS analysis estimates only the chemical composition on the surface, there may be a differential segregation of the active components in the presence of  $K_2CO_3$  as flux. Additionally, in the case of Si and Ca, the difference in the bonding energy before and after the addition of flux was 1.8 and 4 eV, respectively. Usually a change in the bonding energy value of 1 eV indicates a change in the degree of oxidation of the element, however, such a change in the oxidation state is not expected in the compound of Ca and Si, which have a fixed oxidation state of +2 and +4, respectively. At the present we could not figure out the reason for such change, however, the most probable reason could be that some additional phases containing Si, Na and Ca are formed at the surface due to the high-temperature interaction of perlite and  $K_2CO_3$  flux.

Scanning electron microscopy (SEM) was employed to study the induced surface morphological alteration by the heat treatment process. Fig. 3(a) shows the SEM image of perlite powder. The perlite particles show irregular morphology with sharp/broken edges. The morphology of the perlite powders resembles with that of the expanded perlite [17,34]. Fig. 3(b) shows the SEM image of the perlite powder heat-treated at 700 °C without  $K_2CO_3$  flux. When perlite is heated to 700 °C, a temperature higher than its glass transition temperature, the grains start to soften and their edges become blunt/smooth, as can be seen in Fig. 3(b). The microstructure of the unheated perlite powder appears to be composed of agglomerated grains with vast open pores, whereas the microstructure of the heat-treated perlite appears to be dense, compared to that in the unheated perlite, having a network of continuous grains with holes and cells. Fig. 3(c) shows the SEM image of the perlite powder heat-treated at 700 °C with  $K_2CO_3$  flux for 1 h. An extensive coalescence of particles leading to the formation of a dense network with fewer isolated pores can be seen, thus indicating an efficient volume reduction effect of the addition of  $K_2CO_3$  as a flux. The heat-insulating material treated with high-temperature volume reduction has its appearance changed from powder to bulk aggregate-like substance with shiny surface, as shown in Fig. 4.

In order to test the potential adverse effects, if any, of the proposed heat-treatment on the radionuclides present in the perlite-based RTIW, 37.6 ppm Co was added to the perlite- $K_2CO_3$  mixture as a simulated radioactive substance, and the atomic absorption spectroscopy analysis is performed while heating the resulting mix at 1200 °C. Moreover, a calibration curve was constructed by collecting the AAS signals of different Co standards containing 0.5–5 ppm cobalt and data is plotted in Fig. 5, along with the AAS data for the cobalt-containing perlite mixture. As can be seen, the data point for the mixture falls on the trend line and is very close to zero ppm, thus indicating that even heating at 1200 °C the proposed heat-treatment method is able to completely retain all the radionuclide present in the perlite-based RTIW. Moreover, atomic absorption spectroscopy indicates that the proposed heat-treatment procedure is able to completely retain the radionuclides present in the RTIW. In this work, it is observed that by using  $K_2CO_3$  as a flux during thermal treatment of cobalt (Co)-contaminated perlite at relatively lower temperatures a significant volume reduction along with the complete retention of the radionuclide is achieved.

#### 4. Conclusions

In this work, the volume reduction of perlite is studied by high-temperature treatment method while using 0–30 wt%  $K_2CO_3$  as a flux. The differential thermal analysis/thermogravimetric analysis is used to monitor the glass transition temperature ( $T_g$ ) and weight loss. The  $T_g$  shows a minimum at ~643.5 °C with the addition of ~10 wt%  $K_2CO_3$ . In 650–900 °C range, a volume reduction ratio (VRR) of 11.20 is observed at 700 °C with 5 wt%  $K_2CO_3$  as compared to VRR of 5.56 without  $K_2CO_3$ . The X-ray photoelectron spectroscopy and energy dispersive X-ray spectroscopy analyses of perlite samples heat-treated at 700 °C without/with 5 wt%  $K_2CO_3$  are performed for elemental analysis. The scanning electron microscopy is performed to investigate microstructural development leading to the volume reduction by heat-treatment, which indicates an extensive coalescence of particles leading to the formation of a dense network with fewer isolated pores. Moreover, the atomic absorption spectroscopy indicates that the heat-treatment procedure completely retains 37.6 ppm cobalt supposedly present as radionuclides in the radioactive thermal insulation waste.



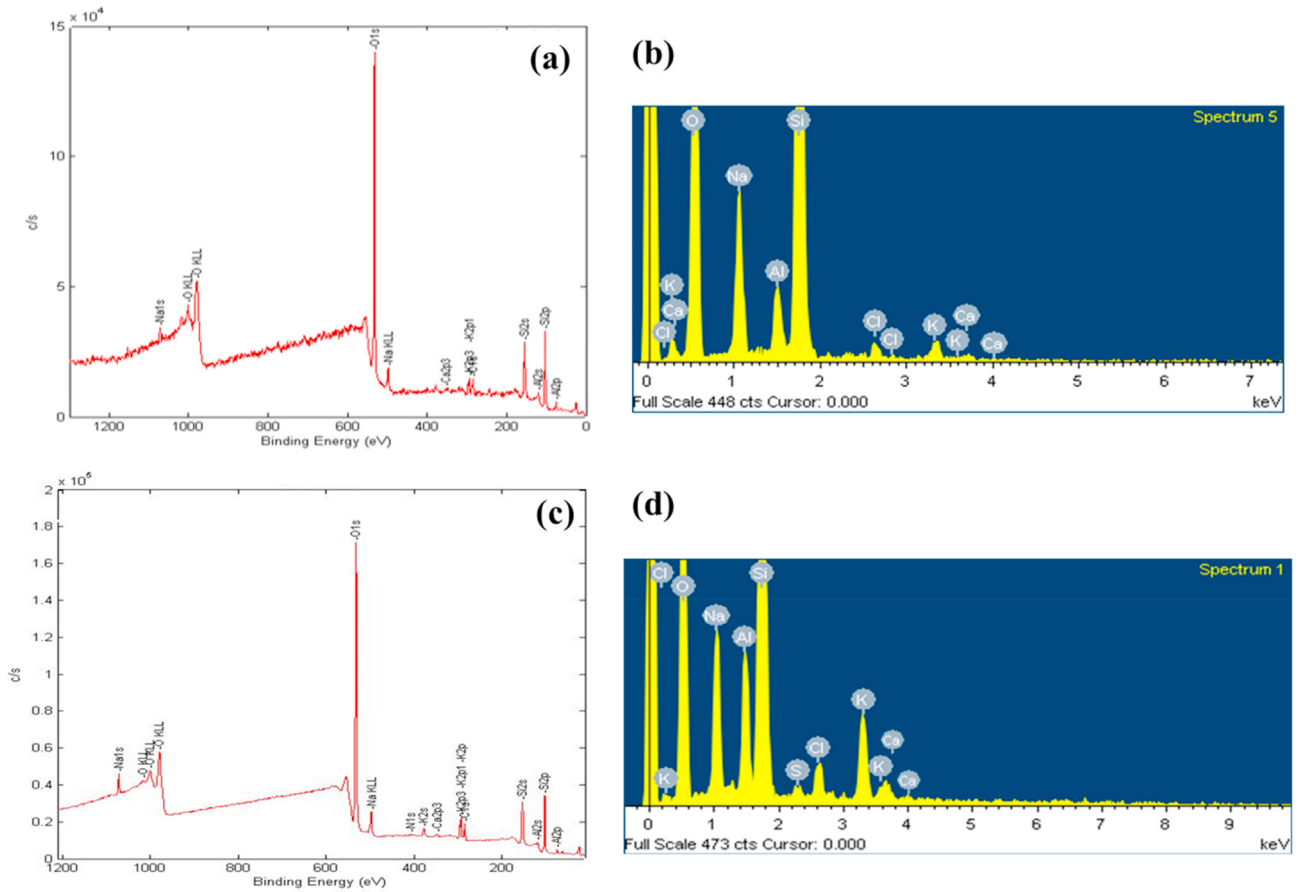


**Fig. 2.** (a) XPS and (b) EDS of powdered perlite sample heat-treated at 700 °C without K<sub>2</sub>CO<sub>3</sub> flux; (c) XPS and (d) EDS of powdered perlite sample heat-treated at 700 °C with 5 wt% K<sub>2</sub>CO<sub>3</sub> flux.

**Table 2**

Binding energy and percentage of elements present on the surface of perlite heat-treated at 700 °C without/with K<sub>2</sub>CO<sub>3</sub> flux.

Constituent	Without K <sub>2</sub> CO <sub>3</sub>		With 5 wt% K <sub>2</sub> CO <sub>3</sub>	
	Binding energy (eV)	Percentage (%)	Binding energy (eV)	Percentage (%)
Si 2p	104.7	23.1	102.9	22.5
O 1s	533.1	61.4	533.4	64.3
Na 1s	1071.4	1.9	1071.1	3.1
C 1s	287.5	8.4	287.0	5.8
K 2p	295.6	1.2	294.8	2.5
Al 2p	75.2	3.8	74.7	1.5
Ca 2p	353.8	0.2	349.8	0.2
N 1s	—	—	407.8	0.1

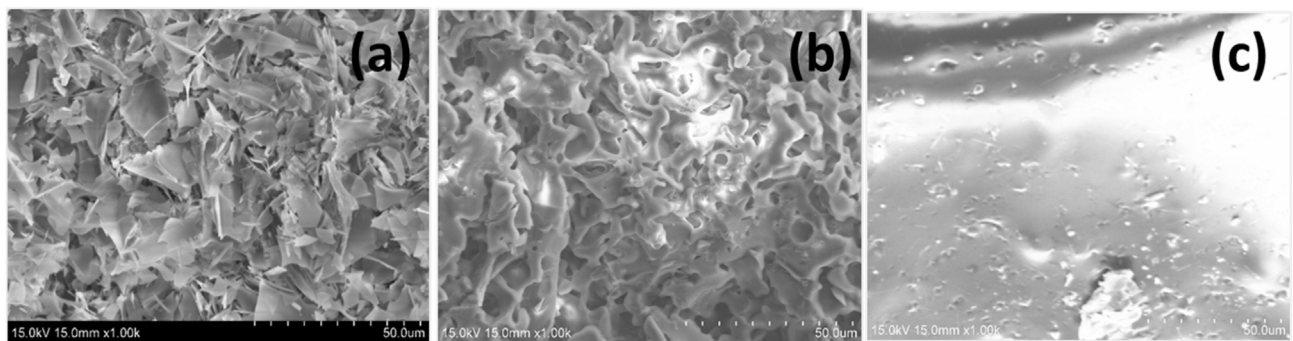


**Fig. 3.** SEM analysis of the surface morphology of pearlite (a) untreated, (b) heat-treated at 700 °C, and (c) raw material added 5 wt% K<sub>2</sub>CO<sub>3</sub> heat-treated at 700 °C for 1 h.

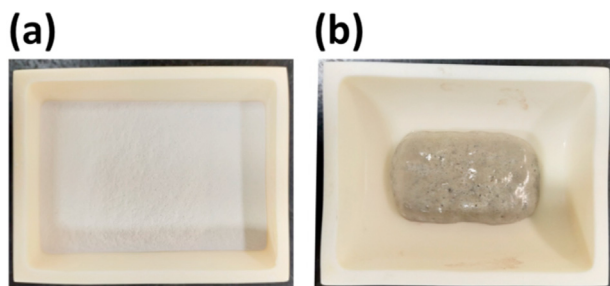


Fig. 4. Appearance of perlite (a) untreated and (b) heat-treated at 700 °C for 1 h with 5 wt%  $K_2CO_3$  flux.

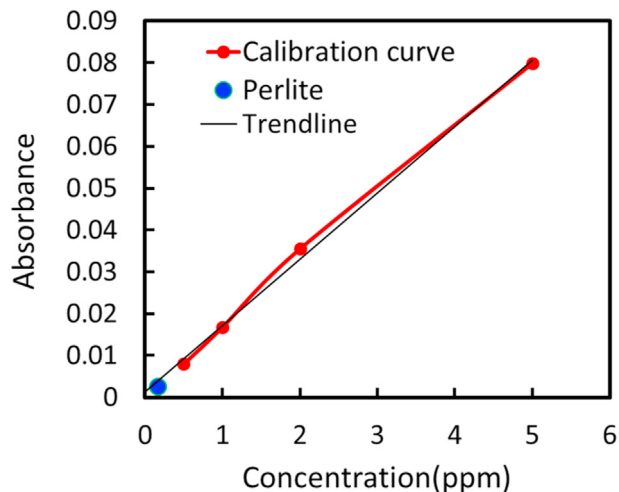


Fig. 5. AAS analysis of the retention of Co in perlite heated at 1200 °C.

## Declaration of competing interest

The authors declare that they have no known competing financial interests or personal relationships that could have appeared to influence the work reported in this paper.

## Acknowledgments

We gratefully thank the financial supports from Fuel Cycle and Materials Administration (FCMA), Atomic Energy Council (AEC) and Institute of Nuclear Energy Research (INER) of Taiwan for the performance of this work under project number: 109FCMA007.

## References

- [1] Radioactive Waste Management <https://www.world-nuclear.org/information-library/nuclear-fuel-cycle/nuclear-wastes/radioactive-waste-management.aspx>.
- [2] M.I. Ojovan, W.E. Lee, S.N. Kalmykov, Treatment of radioactive wastes, in: "An Introduction to Nuclear Waste Immobilisation", Elsevier, 2019, pp. 231–269, <https://doi.org/10.1016/B978-0-08-102702-8.00016-9>.
- [3] R. Kolbe, E. Gahan, Survey of insulation used in nuclear power plants and the potential for debris generation, Albuquerque, NM, and Livermore, CA (United States), <https://doi.org/10.2172/5235578>, 1982.
- [4] N.D. Musatov, V.G. Pastushkov, P.P. Poluektov, T.V. Smelova, L.P. Sukhanov, Compaction of radioactive thermal-insulation materials and construction debris by melting in a cold crucible, *At. Energy* 99 (3) (2005) 602–606, <https://doi.org/10.1007/s10512-005-0253-z>.
- [5] M. Garamszeghy, Compaction processes and technology for treatment and conditioning of radioactive waste, in: Handbook of Advanced Radioactive Waste Conditioning Technologies, Elsevier, 2011, pp. 19–42, <https://doi.org/10.1533/9780857090959.1.19>.
- [6] Iaea Nuclear Energy Series, Status and Trends in Spent Fuel and Radioactive Waste Management, 2018.
- [7] Application of Thermal Technologies for Processing of Radioactive Waste,

- IAEA-TECDOC-1527, Vienna, 2006.
- [8] P. Kovarič, J.D. Navratil, J. John, Scientific and engineering literature mini review of molten salt oxidation for radioactive waste treatment and organic compound gasification as well as spent salt treatment, *Sci. Technol. Nucl. Install.* 2015 (2015) 1–10, <https://doi.org/10.1155/2015/407842>.
- [9] H.-C. Yang, Y.-J. Cho, H.-C. Eun, J.-H. Yoo, J.-H. Kim, Behavior of toxic metals and radionuclides during molten salt oxidation of chlorinated plastics, *J. Environ. Sci. Heal. Part A* 39 (6) (2004) 1601–1616, <https://doi.org/10.1081/ESE-120037857>.
- [10] T.R. Griffiths, V.A. Volkovich, A new technology for the nuclear industry for the complete and continuous pyrochemical reprocessing of spent nuclear fuel: catalyst enhanced molten salt oxidation, *Nucl. Technol.* 163 (3) (2008) 382–400, <https://doi.org/10.13182/NT08-A3997>.
- [11] T.R. Griffiths, V.A. Volkovich, Robert carper, W. The structures of the active intermediates in catalyst-enhanced molten salt oxidation and a new method for the complete destruction of chemical warfare arsenicals, *Struct. Chem.* 21 (2) (2010) 291–297, <https://doi.org/10.1007/s11224-009-9530-0>.
- [12] M.-F. Fan, Risk discourses and governance of high-level radioactive waste storage in taiwan, *J. Environ. Plann. Manag.* 62 (2) (2019) 327–341, <https://doi.org/10.1080/09640568.2017.1418303>.
- [13] Radioactive Waste Management in Taiwan <https://www.aec.gov.tw/english/category/Radioactive-Waste-Management/Radioactive-Waste-Management-in-Taiwan-146.html>.
- [14] First nuclear power plant decommissioning plan. <https://www.taipower.com.tw/en/page.aspx?mid=4506>.
- [15] M. Singh, M. Garg, Perlite-based building materials- A review of current applications, *Construct. Build. Mater.* 5 (2) (1991) 75–81, [https://doi.org/10.1016/0950-0618\(91\)90004-5](https://doi.org/10.1016/0950-0618(91)90004-5).
- [16] I.B. Topçu, B. Işıkdag, Effect of expanded perlite aggregate on the properties of lightweight concrete, *J. Mater. Process. Technol.* 204 (1–3) (2008) 34–38, <https://doi.org/10.1016/j.jmatprotec.2007.10.052>.
- [17] A.A. Reka, B. Pavlovski, K. Lisichkov, A. Jashari, B. Boev, I. Boev, M. Lazarova, V. Eskizybek, A. Oral, G. Jovanovski, P. Makreski, Chemical, mineralogical and structural features of native and expanded perlite from Macedonia, *Geol. Croat.* 72 (3) (2019) 215–221, <https://doi.org/10.4154/gc.2019.18>.
- [18] V. Pavlík, J. Bisaha, Lightweight mortars based on expanded perlite, *Key Eng. Mater.* 776 (2018) 104–117, [10.4028/www.scientific.net/KEM.776.104](https://doi.org/10.4028/www.scientific.net/KEM.776.104).
- [19] V. Blaskov, I. Stambolova, V. Georgiev, T. Batakiev, A. Eliyas, M. Shipochka, S. Vassilev, D. Mehandjiev, Synthesis and catalytic activity of silver-coated perlite in the reaction of ozone decomposition, *Ozone Sci. Eng.* 37 (3) (2015) 252–256, <https://doi.org/10.1080/01919512.2014.983453>.
- [20] M. Dogan, M. Alkan, Some physicochemical properties of perlite as an adsorbent, *Fresenius Environ. Bull.* 13 (2004) 251–257.
- [21] N. Yoshikuni, Novel rapid decomposition and dissolution method for silicates using a mixed potassium metaborate/potassium carbonate flux, *Talanta* 43 (11) (1996) 1949–1954, [https://doi.org/10.1016/0039-9140\(96\)01983-2](https://doi.org/10.1016/0039-9140(96)01983-2).
- [22] R.J. Julietti, D.R. Williams, Versatile fusion method for the dissolution of refractory materials, *106* (1264), *Analyst* 794 (1981), <https://doi.org/10.1039/an9810600794>.
- [23] T. Dulski (Ed.), A Manual for the Chemical Analysis of Metals, 1996, pp. 82–92, <https://doi.org/10.1520/MNL25-EB>. ASTM International: 100 Barr Harbor Drive, PO Box C700, West Conshohocken, PA 19428-2959.
- [24] D.-G. Kim, M.-A. Van Ende, P. Hudon, I.-H. Jung, Coupled experimental study and thermodynamic optimization of the  $K_2O-SiO_2$  system, *J. Non-cryst. Solids* 471 (2017) 51–64, <https://doi.org/10.1016/j.jnoncrysol.2017.04.029>.
- [25] Radiological Characterization of Shut Down Nuclear Reactors for Decommissioning Purposes, Vienna, 1998.
- [26] Management of Radioactive Waste after a Nuclear Power Plant Accident; 2016.
- [27] W.P. Chang, C.C. Chan, J.D. Wang, 60Co contamination in recycled steel resulting in elevated civilian radiation doses: causes and challenges, *Health Phys.* 73 (3) (1997) 465–472, <https://doi.org/10.1097/00004032-199709000-00004>.
- [28] E.A.C. Crouch, Fission-product yields from neutron-induced fission, *at. Data nucl. Data Tables* 19 (5) (1977) 417–532, [https://doi.org/10.1016/0092-640X\(77\)90023-7](https://doi.org/10.1016/0092-640X(77)90023-7).
- [29] Q. Han, Y. Huo, L. Yang, T. Hao, X. Yang, Y. Zhai, Determination of ultra-trace cobalt in water samples by graphite furnace atomic absorption spectrometry after cloud point extraction using 2-(5-Bromo-2-pyridylazo)-5-dimethylaminoaniline as the chelating agent, *anal. Methods* 7 (2015) 8931–8935, <https://doi.org/10.1039/C5AY02088C>.
- [30] N. Bagdassarov, F. Ritter, Y. Yanev, Kinetics of perlite glasses degassing: TG and DSC analysis, *Glastech. Ber. Glass Sci. Technol.* 72 (9) (1999) 277–290.
- [31] P.S. Thomas, K. Heide, M. Foldvari, Water and hydrogen release from perlites and opal, *J. Therm. Anal. Calorim.* 120 (2015) 95–101, <https://doi.org/10.1007/s10973-014-4336-8>.
- [32] R. Karakas, U. Yuksel, Modification of perlite for use as a thin-layer chromatographic adsorbent, *J. Chromatogr. Sci.* 36 (10) (1998) 499–504, <https://doi.org/10.1093/chromsci/36.10.499>.
- [33] A. Chakir, J. Bessiere, K.E. Kacemi, B. Marouf, A comparative study of the removal of trivalent chromium from aqueous solutions by bentonite and expanded perlite, *J. Hazard Mater.* 95 (1–2) (2002) 29–46, [https://doi.org/10.1016/S0304-3894\(01\)00382-X](https://doi.org/10.1016/S0304-3894(01)00382-X).
- [34] M. Giannouri, T. Kalampaliki, N. Todorova, T. Giannakopoulou, N. Boukos, D. Petrakis, T. Vaimakis, C. Trapalis, One-step synthesis of  $TiO_2$ /perlite composites by flame spray pyrolysis and their photocatalytic behavior, *Int. J. Photoenergy* 2013 (2013) 1–8, <https://doi.org/10.1155/2013/729460>.